Available online at www.sciencedirect.com
SCIENCE DIRECT®
Journal of Chromatography A, 1003 (2003) 73–89
JOURNAL OF CHROMATOGRAPHY A
www.elsevier.com/locate/chroma

Study of the competitive isotherm model and the mass transfer kinetics for a BET binary system

Wojciech Piatkowski[a,b,c], Dorota Antos[a], Fabrice Gritti[b,c], Georges Guiochon[b,c,*]

[a]*Faculty of Chemistry, Rzeszów University of Technology, W. Pola 2 Street, 35-959 Rzeszów, Poland*
[b]*Department of Chemistry, University of Tennessee, 414 Buhler Hall, Knoxville, TN 37996-1600, USA*
[c]*Division of Chemical Sciences, Oak Ridge National Laboratory, Oak Ridge, TN 37831-6120, USA*

Received 12 February 2003; received in revised form 17 April 2003; accepted 17 April 2003

Abstract

The competitive adsorption behavior of the binary mixture of phenetole (ethoxy-benzene) and propyl benzoate in a reversed-phase system was investigated. The adsorption equilibrium data of the single-component systems were acquired by frontal analysis. The same data for binary mixtures were acquired by the perturbation method. For both compounds, the single-component isotherm data fit best to the multilayer BET model. The experimental overloaded band profiles are in excellent agreement with the profiles calculated with either the general rate model or the modified transport-dispersive models. The competitive adsorption data were modeled using the ideal adsorbed solution (IAS) theory. The numerical values of the coefficients were derived by fitting the retention times of the perturbation pulses to those calculated using the IAS theory compiled with the coherence conditions. Finally, the elution profiles of binary mixtures were recorded. They compared very well with those calculated. As a characteristic feature of this case, an unusual retainment effect of the chromatographic band of the more retained component by the less retained one was observed. The combination of the General Rate Model and the adsorption isotherm model allowed an accurate prediction of the band profiles.

Keywords: Adsorption isotherms; Frontal analysis; Perturbation chromatography; Mass transfer

1. Introduction

Preparative chromatography is an industrial process which is still in constant evolution. The most commonly used implementation of this process remains batch overloaded elution. Among the more sophisticated approaches, e.g. displacement chromatography, the various recycling methods and simulated moving bed separations, only the last method has attracted a high level of interest because it enhances yields and affords an improved production rate [1,2]. Most of these methods are complex, experimental trials are long and expensive, hence the design of a new chromatographic process should be done using computer-assisted optimization. To be successful, however, this strategy must rely on the accurate prediction of multicomponent band profiles. Several mathematical models are available for the calculation of band profiles in various chromatographic separation techniques [1,3]. All these models, however, require that the multicomponent adsorption isotherms be accurately accounted for.

*Corresponding author. Tel.: +1-865-974-0733; fax: +1-865-974-2667.
E-mail address: guiochon@utk.edu (G. Guiochon).

0021-9673/03/$ – see front matter
doi:10.1016/S0021-9673(03)00726-X

Since preparative chromatography always involves high degrees of overloading, accompanied by strong isotherm non-linear behavior, the acquisition of reliable information concerning the equilibrium thermodynamics of mixtures is a task of major importance. Inaccuracies in the calculation of band profiles originate most often from errors made in the acquisition of equilibrium isotherm data or, more frequently, in the incorrect modeling of these data. At high concentrations, thermodynamic effects dominate kinetic effects in the control of band profiles.

For practical applications, the most attractive approach is the one consisting of estimating the competitive behavior of the components of a mixture on the basis of the single-component isotherms. Unfortunately, the simple procedure of using the competitive form of the isotherm model best accounting for the single-component isotherm behavior of the feed components and deriving the parameters of the competitive model from those of the single-component isotherms does not always give satisfactory results. The determination of at least a few experimental competitive isotherm data is necessary, possibly to determine some interaction parameters, always to validate the approach. The method becomes difficult to implement when the single-component isotherms of the feed components are not compatible and more multicomponent equilibrium data are necessary. The determination of equilibrium isotherm data for mixtures is a complex task. It involves laborious experiments, which must be performed for mixtures of various relative compositions.

The experimental methods of determination of the adsorption isotherms can be divided into two groups [1,3]: the static and the dynamic methods. The latter are limited to frontal analysis (FA) [1] and the perturbation method [4,5]. These methods exploit the information content of dynamic concentration profiles.

In this work we report on the measurement, the modeling, and the validation of the binary isotherms of two compounds, phenetole and propyl benzoate, which have been selected for exhibiting complex, multilayer adsorption in a conventional packed RPLC system. The thermodynamics and the mass transfer kinetics of homologous compounds that exhibit a similar multilayer adsorption behavior (e.g. butyl benzoate) in the same system has been analyzed previously [6–8]. The easy part, the measurement, modeling, and validation of the single-component isotherm behavior was investigated. We address here the more complex, competitive isotherm behavior. The single-component isotherms were measured by frontal analysis and were easily modeled with the BET isotherm. It was found easier to acquire the competitive isotherm data with the perturbation method [1,5,7,11,12]. The perturbation pulses are easily recorded and their retention times measured accurately. These times, however, do not supply directly an isotherm. An isotherm model must be selected. Then, the numerical parameters of the model are derived from these retention times, using a best fitting approach. The competitive equilibrium isotherm model was determined using the ideal adsorbed solution (IAS) theory [9]. This theory was initially derived by Radke and Prausnitz for gas–solid adsorption [10]. It was modified later for liquid–solid adsorption from dilute solutions [9,10] and implemented by Seidel-Morgenstern and Guiochon [13] to account for the competitive adsorption behavior of the enantiomers of Tröger's base on cellulose triacetate that have most different two-single-component isotherms. In order to validate this isotherm model, overloaded chromatographic band profiles were recorded and compared to the results of calculations performed with this model and the general rate and the modified transport-dispersive models.

2. Theory

After a brief presentation of the models used for the calculation of the elution band profiles, we discuss the measurement and modeling of the equilibrium isotherm models that play a considerable role in this study.

2.1. Modeling of high-performance liquid chromatography

In this work, we used two different models to calculate the band profiles. For the single-component band profiles, we used the general rate (GR) model. For the multicomponent band profiles, we used the transport-dispersive (TR) models.

2.1.1. Modeling for single-component system—general rate model

The GR model used in this work has already been described in detail previously [8,14–16]. So, we give here only a short description of this model. In writing the equations of this model, we made several assumptions that were examined in detail elsewhere [8], in particular:

(1) The influence of the external mass transfer resistances can be ignored.
(2) The influence of surface diffusion can be ignored.

With these assumptions, the differential mass balance for the species in the mobile phase can be expressed as follows:

$$\epsilon_e \cdot \frac{\partial C}{\partial t} + u \cdot \frac{\partial C}{\partial x} = \epsilon_e \; D_L \cdot \frac{\partial^2 C}{\partial x^2} - (1-\epsilon_e) \cdot \frac{\partial \overline{C}_p}{\partial t} \tag{1}$$

where:

$$\overline{C}_p = \frac{3}{R_p^3} \cdot \left[\int_0^{R_p} \epsilon_p C_p r^2 \, dr + \int_0^{R_p} (1-\epsilon_p) q r^2 \, dr \right] \tag{2}$$

where C and C_p are the solute concentrations in the mobile and the stagnant liquid phase, respectively, q is its concentration in the solid-phase, x is the distance along the column, t is time, r is the distance from the particle center, R_p is the particle radius, ϵ_e is the external porosity of the bed, ϵ_p is the mesopore porosity of the particles, u is superficial velocity of the mobile phase, and D_L is the axial dispersion coefficient calculated from the Gunn equation [17].

The mass balance equation for the species in the stagnant liquid phase, within the pores of the particles, can be formulated as:

$$\epsilon_p \cdot \frac{\partial C_p}{\partial t} + (1-\epsilon_p) \cdot \frac{\partial q}{\partial t} = \frac{1}{r^2} \cdot \frac{\partial}{\partial r} \cdot \left[D_{eff} \, r^2 \cdot \frac{\partial C_p}{\partial r} \right] \tag{3}$$

where D_{eff} is the pore diffusion coefficient. If pore diffusion dominates the kinetics of internal mass transfer mechanism, the effective diffusion coefficient, D_{eff}, can be expressed as [1,8]:

$$D_{eff} = D_p \epsilon_p = \frac{\epsilon_p}{\theta} \cdot D_m = \frac{\epsilon_p^2}{(2-\epsilon_p)^2} \cdot D_m \tag{4}$$

where the pore diffusivity, D_p, can be correlated with the molecular diffusivity D_m and the pore tortuosity, θ, given by:

$$\theta = \frac{(2-\epsilon_p)^2}{\epsilon_p} \tag{5}$$

This model is complemented by a set of initial and boundary conditions. For $t = 0$, the initial concentrations are:

$$C(0, x) = 0 \quad \text{for} \quad 0 < x < L \tag{6}$$

$$C_p(0,x,r) = 0 \;\text{ and }\; q(0,x,r) = 0 \quad \text{for} \quad 0 < x < L \;\text{ and }\; 0 < r < R_p \tag{7}$$

The boundary conditions for the first mass balance equation (Eq. (1)) are:

(a) For $t > 0$, at $x = 0$,

$$u_f[C_f(t) - C_f(t,0)] = \epsilon_e D_L \cdot \frac{\partial C(t,0)}{\partial x}$$

with

$$C_f = \begin{cases} C_f & \text{for } t[0;t_p] \\ 0 & \text{for } t > t_p \end{cases} \tag{8}$$

(b) For $t > 0$, at $x = L$,

$$\frac{\partial C}{\partial x} = 0 \tag{9}$$

These Eqs. (8) and (9) represent the Danckwerts conditions [1].

The boundary conditions for the second mass balance equation (Eq. (3)) are:

(a) For $t > 0$, at $r = R_p$,

$$C_p(t, r = R_p) = C \tag{10}$$

(b) For $t > 0$, at $r = 0$,

$$\frac{\partial C_p(t,r)}{\partial r} = 0 \tag{11}$$

2.1.2. Modeling for binary mixtures—transport-dispersive model

For the mathematical modeling of the chromatographic profiles of binary mixtures, we used the TD

model [1,18–20]. In this model, all the contributions of different origins to the mass transfer kinetics are lumped into a single mass transfer rate coefficient, k_m. The TD model consists in one differential mass balance equation for each component, i, in the mobile phase. This equation is written [21]:

$$\frac{\partial C_i}{\partial t} + F \cdot \frac{\partial q_i}{\partial t} + u \cdot \frac{\partial C_i}{\partial x} = \frac{\epsilon_e}{\epsilon_T} \cdot D_L \cdot \frac{\partial^2 C_i}{\partial x^2} \tag{12}$$

where F is the phase ratio, with $F = (1 - \epsilon_T)/\epsilon_T$ and ϵ_T is the total porosity of the bed.

The initial and boundary conditions are similar to those of the GR model [22].

The differential $\partial q_i/\partial t$ is given by the following kinetic equation:

$$\frac{\partial q_i}{\partial t} = k_{m,i}\left[q_i^*(\bar{C}) - q_i\right] \tag{13}$$

where C_i and q_i are the local mobile and stationary phase concentrations, $q_i^*(\bar{C})$ is the equilibrium concentration provided by the competitive isotherm equations, $k_{m,i}$ is the lumped mass transport coefficient which accounts for the contributions of the internal and the external mass transfer resistances and is related as follows to the characteristics of the system [16,23]:

$$\frac{1}{k_m} = A_1 \cdot \frac{\epsilon_e}{\epsilon_T F_e} \cdot \left[\frac{d_p}{6k_{ext}} + \frac{d_p^2}{60D_{eff,i}}\right] = A_1 \cdot \frac{\epsilon_e}{\epsilon_T F_e} \cdot \frac{1}{6k_{ov,i}a_p} \tag{14}$$

with

$$\frac{1}{k_{ov,i}a_p} = \frac{1}{k_{ext}} + \frac{d_p}{10D_{eff,i}} \quad a_p = \frac{6}{d_p} \quad F_e = \frac{1 - \epsilon_e}{\epsilon_e}$$

If the external mass transport resistance is ignored, k_{ov} is directly correlated with the effective diffusion coefficient with $k_{ov,i} = 10D_{eff,i}/d_p$, where $D_{eff,i}$ can be calculated using Eq. (4). The value of k_{ov} is constant, providing that D_{eff} does not vary with the concentration. It can be evaluated by matching the experimental chromatogram recorded under linear conditions and the corresponding calculated chromatogram. The coefficient A_1 is concentration dependent, with:

$$A_1 = k'_{0,i} \cdot \frac{\left(\frac{k_1}{1+k_1}\right)_i^2}{\left(\frac{k'_0}{1+k'_0}\right)_i^2} \tag{15}$$

For a linear isotherm, A_1 is constant. For nonlinear isotherms, the values of $k_{1,i}$ and $k'_{0,i}$ are concentration dependant through the isotherm chord [16,23], with:

$$k_{1,i} = F_2 \cdot \left[\epsilon_p + (1 - \epsilon_p) \cdot \left(\frac{\Delta q^*}{\Delta C}\right)_i\right] \tag{16}$$

$$k'_{0,i} = F \cdot \left(\frac{\Delta q^*}{\Delta C}\right)_i \tag{17}$$

with $\Delta q^*/\Delta C$ the slope of the isotherm chord.

Thus, the lumped mass transport coefficient, k_m cannot be assumed to remain constant, particularly for strong concentration gradients, i.e. when the band profile is steep, a rather frequent occurrence in preparative HPLC. The influence of the concentration dependence of the model predictions made under different experimental conditions has been thoroughly analyzed previously [23,24]. In order to calculate the profiles of chromatographic bands, the following approximation of the isotherm chord by the isotherm slope is suggested [24]:

$$\frac{\Delta q_i^*}{\Delta C_i} = \frac{\partial q_i^*}{\partial C_i} \tag{18}$$

This approximation was found to give good results even for very low column efficiency [15] and for complex mass transfer mechanisms, involving surface diffusion [16]. In order to determine k_m from the dispersed fronts of breakthrough fronts, the local slope of the isotherm should be used [1,15,23]:

$$k_{1,i} = F_e \cdot \left[\epsilon_p(1 - \epsilon_p) \cdot \left(\frac{\partial q^*}{\partial C}\Big|_{\bar{C}}\right)_i\right] \tag{19}$$

$$k'_{0,i} = F \cdot \left(\frac{\partial q^*}{\partial C}\Big|_{\bar{C}}\right)_i \tag{20}$$

In this case, the lumped coefficient k_m depends on the local concentration, $\bar{C}$. Including all the above relationships (Eqs. (4), (19)–(21)), the lumped mass transfer coefficient, k_m of component i can be expressed as:

$$k_{m,i} = \frac{60F_e\epsilon_e}{d_p^2} \cdot \frac{A_{1,i}\epsilon_p^2 D_{m,i}}{(2-\epsilon_p)^2\epsilon_T} \quad (21)$$

where A_1 is obtained from Eq. (15).

2.2. Adsorption equilibrium for single component

The equilibrium isotherm data of the two pure compounds studied here were measured by frontal analysis (FA) and modeled. These data were found to fit well to a BET isotherm.

2.2.1. Measurement of the adsorption isotherm data for single-component by frontal analysis

Frontal analysis is considered to be the most accurate and reliable method of measurement of the isotherm data [1,6–8,39]. In this work, this method was used for the pure compounds and the isotherm data were derived from the following integral mass balance equation:

$$q^*(C_F) = \frac{C_F(V_{eq} - V_0)}{V_a} \quad (22)$$

where V_{eq} and V_0 are the elution volume of the equivalent area of the front of a concentration plateau at $C = C_F$, and the hold-up volume, respectively, and V_a is the volume of stationary phase in the column.

2.2.2. Modeling of single-component isotherm data

The BET isotherm model, which assumes multilayer adsorption [25,26], was found to provide the best fit to the adsorption isotherm data of both phenetole and propyl benzoate. This model was developed to describe adsorption phenomena in which successive molecular layers of adsorbate form at pressures well below the pressure required for completion of the monolayer. The same model was used for the homologous compound in Refs. [6–8] (butyl benzoate). The isotherm equation can be expressed as follows:

$$q_i^* = \frac{q_{s,i} b_{s,i} C_i}{(1 - b_{L,i}C_i)(1 - b_{L,i}C_i + b_{s,i}C_i)} \quad \text{with} \quad i = 1,2,\ldots,n \quad (23)$$

where $q_{s,i}$ is the monolayer saturation capacity of the adsorbent for component i; b_S is the equilibrium constant for surface adsorption–desorption (i.e. over the free surface of the adsorbent) and b_L is the equilibrium constant for surface adsorption–desorption over a layer of adsorbate molecules.

The local slope of the BET isotherm is used in Eqs. (16) and (18). It is given by:

$$\frac{\Delta q_i^*}{\Delta C_i} \equiv \frac{\partial q_i^*}{\partial C_i} = q_{s,i} b_{s,i} \cdot \frac{1 - b_{L,i}^2 C_i^2 + b_{S,i} b_{L,i} C_i^2}{(1 - b_{L,i}C_i)^2 (1 - b_{L,i}C_i + b_{S,i}C_i)^2} \quad (24)$$

In the case of the corresponding competitive isotherm model, the local isotherm slope for component i is calculated using the IAS theory, see Section 2.4.2.

2.3. Isotherm model for binary-component system. Competitive isotherm model

The competitive isotherm data were measured by the perturbation method because it is easier to implement than frontal analysis.

2.3.1. Perturbation method

In the perturbation method [27,28], the column is initially equilibrated with a percolating solution of the mixture studied in the mobile phase, at a known concentration level. Then, a small perturbation is introduced as a positive or negative rectangular concentration pulse. Since the perturbation is small, the column remains in equilibrium with the mobile phase. The operation is repeated for increasing concentration levels and the retention times of the pulses are measured and analyzed. The mathematical analysis is based on the principle of the classical equilibrium theory [12,29]. Using the column mass balance equation and the coherence condition [29], the following equations can be derived:

$$t_{r,i,k} = \frac{\epsilon_T V_{col}}{\dot{V}} \left(1 + F \cdot \frac{dq_i^*}{dC_i}\Big|_{\bar{C}}\right) = t_0 \left(1 + F \cdot \frac{dq_i^*}{dC_i}\Big|_{\bar{C}}\right) \quad \text{for } i = 1,\ldots,n \text{ and } k = 1,\ldots,n \quad (25)$$

where $\bar{C}$ is the vector of the C_i concentrations. For

$n = 2$, the differentials dq_i^*/dC_i are the two directional derivatives:

$$\frac{dq_i^*}{dC_i}\Big|_{\bar{C}} = \sum_{k=1}^{n} \frac{\partial q_i^*}{\partial C_j}\Big|_{\bar{C}} \frac{dC_j}{dC_i}\Big|_{\bar{C}} \tag{26}$$

The partial derivatives, $\partial q_i^*/\partial C_j$ can be explicited on the basis of the competitive isotherm model. The derivatives dC_j/dC_i can be calculated as the two roots of the equation resulting from the coherence condition [1,5]:

$$\left(\frac{dC_1}{dC_2}\Big|_{\bar{C}}\right)_{\pm} = -\frac{\left(\frac{\partial q^*}{\partial C}\right)_2\Big|_{\bar{C}} - \left(\frac{\partial q^*}{\partial C}\right)_1\Big|_{\bar{C}}}{2\frac{\partial q_2^*}{\partial C_1}} \pm \sqrt{\left[\frac{\left(\frac{\partial q^*}{\partial C}\right)_2\Big|_{\bar{C}} - \left(\frac{\partial q^*}{\partial C}\right)_1\Big|_{\bar{C}}}{2\frac{\partial q_2^*}{\partial C_1}}\right]^2 + \frac{\frac{\partial q_1^*}{\partial C_2}\Big|_{\bar{C}}}{\frac{\partial q_2^*}{\partial C_1}\Big|_{\bar{C}}}} \tag{27}$$

This equation leads to the two retention times $t_{R,11} = t_{R,21}$ and $t_{R,12} = t_{R,22}$.

2.3.2. Competitive isotherm model

To describe the competitive adsorption isotherms, the IAS theory was used. This theory allows the calculation of the competitive adsorption isotherm of the components of mixtures from their single-component isotherms without the need for additional parameters [9,10]. The IAS theory assumes that a modified spreading pressure for each of single solute is equal to:

$$\pi_i(C_i^0) = \int_0^{C_i^0} \frac{q_i^*(C_i)}{C_i}\, dC_i \tag{28}$$

where the values C_i^0 are fictitious concentrations of the pure compound that would give the same spreading pressure π as that of the mixture:

$$\pi_i(C_i^0) = \pi_{\text{mixture}} \tag{29}$$

From Raoult's law, the equilibrium relationships are written:

$$C_i = x_{s,i} C_i^0 \tag{30}$$

with:

$$\sum_{i=1}^{n} \frac{C_i}{C_i^0} = 1 \tag{31}$$

where $x_{s,i}$ is the mole fraction of solute i in the solid-phase.

The equilibrium coefficient between layers that have already been adsorbed should reflect the fact that adsorption can take place in any of the underlying layers [30]. In order to calculate the equilibrium constant between successive layers ($\bar{b}_{L,i}$), the geometric mean rule was applied:

$$B_{L,i,j} = B_{L,j,i} = \sqrt[n]{\Pi_j^n b_{i,j}}; \quad B_{L,i,i} = B_{L,i}$$
$$\bar{b}_{L,i} = \sum_j B_{L,i,j}\, x_{s,i}. \tag{32}$$

In order to calculate C_i^0 and $x_{s,i}$, the set of Eqs. (28)–(32) must be solved numerically. The competitive equilibrium isotherms can then be calculated using the single-component isotherms for total equilibrium loading:

$$\frac{1}{q_{\text{tot}}^*} = \sum_{i=1}^{n} \frac{x_{s,i}}{q_i^*(C_i^0)} \tag{33}$$

The stationary concentration of each solute species in the mixture is calculated from:

$$q_i^* = x_{s,i} q_{\text{tot}}^* \tag{34}$$

As a result of these calculations, it is possible to derive the stationary phase concentrations of each component of a mixture when their single-component isotherms are known. It should be noted, however, that the perturbation method gives the retention times of the pulses, not the explicit values of the stationary phase concentrations.

2.4. Numerical solution of the GR and TD models

2.4.1. General rate model

The GR model has no closed-form solutions. Numerical solutions were calculated using a computer program based on an implementation of the method of orthogonal collocation on finite elements [1,31–34]. The set of discretized ordinary differential equations was solved by the Adams–Moulton method, implemented in the VODE procedure [35]. The relative and absolute errors of the numerical calculations were $1 \cdot 10^{-6}$ and $1 \cdot 10^{-8}$, respectively.

2.4.2. The transport-dispersive model

The TD model used for the calculation of band profiles of binary mixtures was solved numerically, using a finite difference (the backward–forward method). The time increment was chosen in such a way that the numerical diffusion was negligible. The validity of the numerical solutions obtained was verified by comparing them to the solutions obtained with the general model in the case of single-component band profiles. Since no differences were observed between the profiles calculated by either method, the binary mixture elution profiles were calculated with the IAS isotherm model and the finite difference scheme of the TD chromatography model.

3. Experimental

3.1. Chemicals

The same mobile phase was used in this work for the determination of the adsorption isotherm data, for the elution of the perturbation peaks, and for the acquisition of large size band profiles. It is a mixture of HPLC-grade water–methanol (35:65, v/v), both purchased from Fisher Scientific (Fair Lawn, NJ, USA). The solvents used to prepare the mobile phase were filtered before use on an SFCA filter membrane, 0.2 Å pore size (Suwannee, GA, USA). Uracil, phenetole (ethoxy-benzene) and propyl benzoate were obtained from Aldrich (Milwaukee, WI, USA).

3.2. Materials

The packed column is a Symmetry C_{18} column, 150×3.9 mm, endcapped (Ref. No. 2 Waters, Milford, MA, USA). This column belonged to the lot of 15 columns used by Kele and Guiochon [36] for their study of the repeatability of the chromatographic properties of these columns. The hold-up time of this column was determined from the retention time of uracil injections. For a mobile phase composition water–methanol (35:65, v/v), the elution time of uracil is similar to that of methanol or sodium nitrate and gives an excellent estimate of the column void volume. The mean of at least five consecutive readings, agreeing to within 1% was taken for each plateau concentration of the mobile phase (see Table 1).

Table 1
Physico–chemical properties of the packed silica column No. 2 [34]

Packed column	
Diameter of column d_c	3.9 mm
Length of column L	150 mm
Column volume V_c	1.791 (ml)
Particle size d_p	5 μm
$a_p = 6/d_p$	12 000 (1/cm)
Skeleton size	1.3–1.5 μm
Interparticle size	1.25–2 μm
Mesopore size	90 Å
Surface area (before C_{18} bonding)	340 m^2/g
Surface coverage (C_{18})	3.2 μmol/m^2
Total carbon	18%
Endcapping	Yes
t_{0s1} (dead time of the system without column-delivery system)	0.31 min
t_{0s2} (dead time of the system without column-syrengine)	0.057 min
Dead time t_0 (column)	1.093 min

The physico–chemical properties of the column supplied by the manufacturer are listed in Table 1. The external porosity of the column was obtained from Ref. [37] ($\epsilon_e = 0.37$).

3.3. Apparatus

The data were acquired using a Hewlett–Packard (now Agilent Technologies, Palo Alto, CA, USA) HP 1090 liquid chromatograph. This instrument includes a multi-solvent delivery system (tank volume, 1 l each), an auto-sampler with a 25 μl loop, a diode-array UV-detector, a column thermostat and a computer data acquisition station. Compressed nitrogen and helium bottles (National Welders, Charlotte, NC, USA) are connected to the instrument to allow the continuous operation of the pump and the auto-sampler. The extra-column volumes are 0.057 and 0.310 l as measured from the auto-sampler and the pump system, respectively. All the retention data were corrected for this contribution. All measurements were carried out at a constant temperature of 23 °C.

3.4. Frontal analysis measurements of single-component isotherms

Just prior to the acquisition of each series of single-component isotherm data, a calibration curve was recorded for the solute at the wavelengths of 280, 287, and 293 nm. Adsorption data for 37 concentrations were acquired, uniformly distributed across the concentration range investigated (0.2 to 15 g/l). The non-linear calibration data fitted very well to a third-degree polynomial.

One pump of the HPLC instrument was used to deliver a stream of the pure mobile phase, the second pump, a stream of pure sample solution. The desired concentration of the studied compound was obtained by selecting the concentration of the mother sample solution and the flow-rate fractions delivered by the two pumps. The breakthrough curves were recorded successively, all at a flow-rate of 1 ml/min, with a time delay between each successive breakthrough curve that was sufficiently long to allow for the reequilibration of the column with the pure mobile phase. The injection time of the sample depends on the time required to reach the plateau concentration at the outlet of the column.

The retention volumes of small pulses of uracil were determined from the average of five successive injections made at different plateau concentrations, from 0.2 to 15 g/l, by step of about 0.3 g/l. The overloaded single-component profiles further used for the validation of the isotherm model and to evaluate kinetic effects were recorded at wavelengths of 287 and 293 nm for phenetole (1), and at 293 nm for propyl benzoate (2).

3.5. Perturbation measurements of single- and binary-component isotherms

The major goal of this work was to provide accurate competitive isotherm data and a correct model of these data for the two compounds studied, phenetole and propyl benzoate. Hence, perturbation measurements were made at constant plateau concentrations. This method has the disadvantage of requiring large volumes of the pure mobile phase, hence the frequent, reproducible preparation of large volumes of methanol–water (65:35, v/v). Great care must be taken during the preparation of the mobile phase. Otherwise, a significant error in the measurement of the elution time of the perturbation peaks would take place each time a new solution was used, and the isotherm data obtained by frontal analysis and perturbation methods would not be consistent. We prepared for each plateau 3.6 l of the pure mobile phase (2.34 l of methanol + 1.26 l of water, the water being always poured into the methanol). In 1 l of the eluent, we dissolved 15 g of each of the two probe compounds, phenetole (1) and propyl benzoate (2) which gave the two mother solutions used. These solutions were placed in an ultrasonic bath for 10 min, for degassing.

To obtain the desired plateau concentration, the step gradient mode of the equipment is used as explained in the previous section, for the FA measurements. The binary breakthrough curves are recorded successively, at a flow-rate of 1 ml/min, with a sufficiently long time delay between each breakthrough curve to allow enough time for the reequilibration of the column with the pure mobile phase. Two series of data acquisition were performed, at 36 different plateau concentrations or compositions.

(a) for 1:1 mixtures, the concentration of each compound was increased in the range from $C_{i,\min} = 0.26$ g/l to $C_{i,\max} = 12.56$ g/l for each compound.
(b) for mixtures of variable relative composition but with a total concentration $C_{\text{total}} = C_1 + C_2 = 15$ g/l the initial composition was $C_1 = 0.3$, $C_2 = 14.7$ g/l and the final composition $C_1 = 14.7$ and $C_2 = 0.3$ g/l.

Samples of 10 μl of a dilute solution of uracil in the pure mobile phase were injected, providing a negative perturbation. In order to perform correctly the measurements of the retention times of the perturbation pulses and to obtain for them peaks with profiles as close to gaussian as possible, it is important to record the chromatograms at the highest possible signal/noise ratio of the detector. The signal for the solutes was recorded at wavelengths of 280 (for uracil), 287 and 293 nm for the two compounds. At the highest concentrations used, such perturbations might not be linear any longer and their peak profiles may no longer be gaussian, due to the non-linear behavior of the isotherm. So, the pulse size was adjusted and optimized so that the measure-

ments of the width and retention time of the perturbation signal was accurate enough.

The overloaded profiles obtained upon injection of large samples of mixtures of the two components were recorded separately. These profiles were generated with mixtures of different compositions: 1:2; 1:1 and 2:1, and a maximum concentration of either component 1 or 2 of about 15 g/l. They were recorded at wavelengths of 287 and 293 nm and were used for the validation of the models of the competitive isotherms and of the mass transfer kinetics that we had developed.

4. Results and discussion

In a previous report [6–8], we investigated the single-component adsorption behavior of a similar compound, butyl benzoate, on a monolithic and a packed column, with methanol–water as the mobile phase. We showed that the adsorption data measured for this compound fitted well to the liquid–solid extended BET isotherm model. The GR model of chromatography was used successfully to calculate chromatographic band profiles while using the same value of the molecular diffusivity, D_m, for all sample sizes [8]. Butyl benzoate was replaced by propyl benzoate in this study in order to provide stronger interference with phenetole. The criteria for the selection of these two compounds were:

(a) A relatively small value of the separation factor (less than 1.3);
(b) The same single-component isotherm model, the BET;
(c) Reasonable UV-detector response at different wavelengths, providing accurate measurements of the profiles of the perturbation pulses (sensitivity) yet allowing the record of accurate concentration profiles for large size samples.

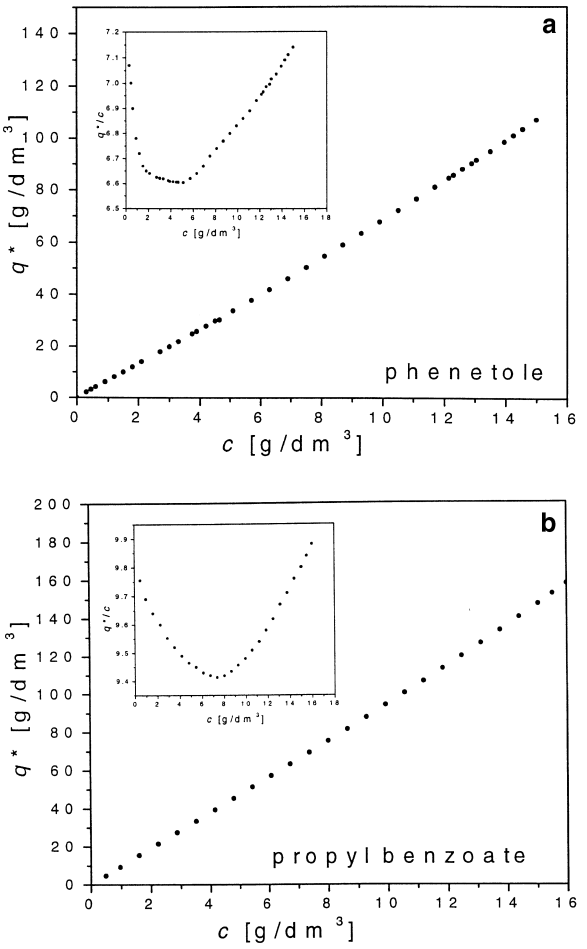

Fig. 1. Plots of the single-component isotherm data obtained by the FA method. Symmetry C_{18} packed column, methanol–water (65:35, v/v), $T=295$ K. Inserts: plots of q^*/C versus C. (a) Phenetole. (b) Propyl benzoate.

4.1. Measurements of the total and internal column porosities and of single-component isotherms

The total porosity of the column used (column No. 2, Refs. [6–8,37]) was derived from the retention

Table 2
BET isotherm model parameters for single-component systems

Compound	Fisher	q_s	IC_{95} (%)	b_S	IC_{95} (%)	b_L	IC_{95} (%)
Phenetole (1)	$8.223\cdot10^4$	188.00	4.6	0.03484	3.4	0.01791	1.8
Propyl benzoate (2)	$1.128\cdot10^5$	138.35	3.0	0.06975	2.6	0.02412	0.7

time of uracil in the mobile phase. This retention time decreases with increasing concentration of the plateau concentration, an effect which was assumed to originate from a decreasing pore volume due to the multilayer adsorption that takes place for compounds that exhibit BET isotherm behavior. In previous studies, we observed this effect and corrected the model of chromatography to account for it [7,8]. If the mesopore porosity is assumed to be constant, the total porosity changes with the solute concentration. The variation of the porosity can be expressed by an empirical equation:

$$\epsilon_{T,i} = \epsilon_T^0 - \lambda_i C_i \quad (35)$$

where C_i is the concentration of compound i. When a mixture of the two compounds is used, C_i in Eq. (35) should be $C_i = C_{total}$. The numerical coefficient λ_i is an empirical parameter, with values given in Table 3. The macropore and the mesopore porosities of the

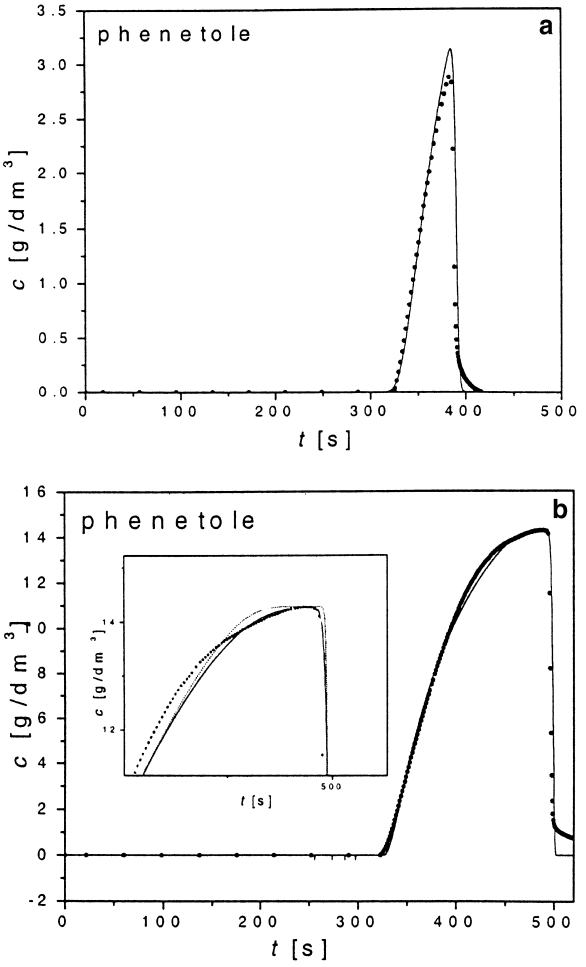

Fig. 2. Comparison between calculated and experimental band profiles for pure phenetole. Validation of the BET isotherm model. Profiles calculated with the GR model. $D_m = 5.46 \cdot 10^{-6}$ cm^2/s. (a) $C_0 = 3.755$ g/ml; $t_p = 30$ s; $L_f = 0.91\%$. (b) $C_0 = 14.496$ g/ml; $t_p = 120$ s; $L_f = 14.12\%$. Insert: enlarged profiles. Solid line, profile calculated with the concentration dependence of the total porosity; dashed line, profile calculated with a constant total porosity.

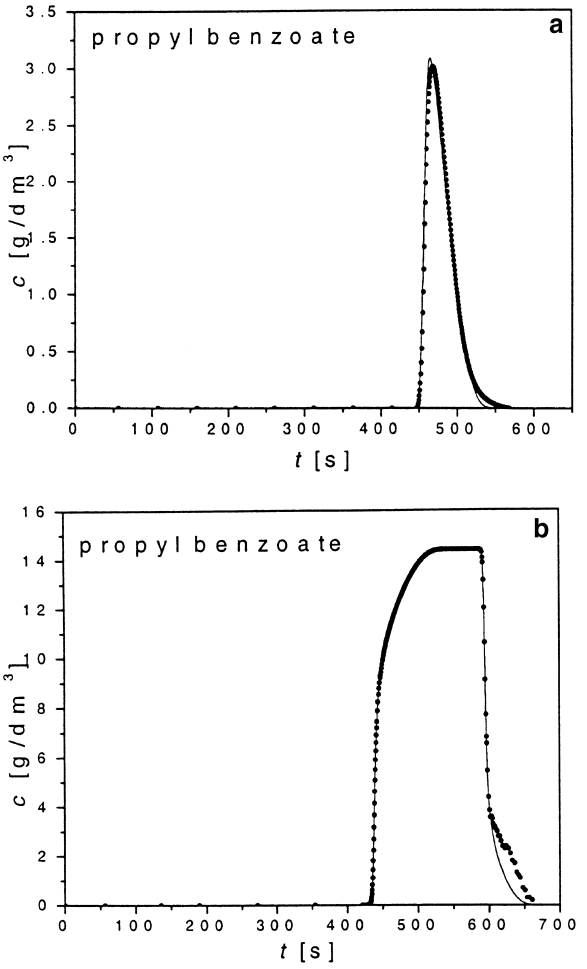

Fig. 3. Comparison between calculated and experimental band profiles for pure for propyl benzoate. Validation of the BET isotherm model. Profiles calculated with the GR model. $D_m = 4.87 \cdot 10^{-6}$ cm^2/s. (a) $C_0 = 3.755$ g/ml; $t_p = 30$ s; $L_f = 1.24\%$. (b) $C_0 = 14.496$ g/ml; $t_p = 120$ s; $L_f = 19.18\%$.

adsorbent depend on the adsorbate concentration for both compounds, much as was described in Refs. [7,8], but unlike what was observed with the monolithic column, the dependence of the porosities of the solute concentrations observed with this conventional packed column is weak (see Table 3).

The isotherm data obtained for either compounds fit extremely well to the same single-component isotherm model, the BET model [6–8] (see Table 2, Fisher coefficients of the order of $1 \cdot 10^5$ and Fig. 1a and b). The best values of the parameters of the isotherm model were calculated from the breakthrough curves. They are reported in Table 2. The values of these parameters, q_s, b_S, and b_L calculated with and/or without taking into account the effect of the variation of the total porosity with the solute concentration differ by less than 0.67% for both compounds. So, we neglected this dependence in the rest of this work and in the interpretation of our results, which causes only a small error in the modeling of the band profiles (see Fig. 2b).

4.2. Validation of the isotherm model for the single components

A series of overloaded band profiles for single-component samples were acquired in which the experimental conditions were varied systematically. These profiles were compared to those calculated using the GR and the TD models and the BET isotherm. The lumped mass transfer rate coefficient, $k_{m,i}$ was found to be practically proportional to D_{eff} for both compounds. It is given by Eq. (22). The molecular diffusivity, $D_{m,i}$, for both compounds was calculated from the Wilke and Chang equation [6–8,40]. Some examples are given in Figs. 2a and b and 3a and b.

For both compounds, the single-component BET isotherm model, with a constant effective diffusion coefficient, D_m, given by Eq. (4) allows the accurate prediction of the band profiles over the range of loading factors that was investigated, $0.002 < L_f < 0.20$ (or between 0.2 and 20%). The loading factor is defined as the ratio of the amount injected to the saturation capacity of the column. The other parameters of the GR and TD models were calculated and are reported in Table 3. In Fig. 2a and b (phenetole) and in Fig. 3a and b (propyl benzoate), overloaded elution band profiles obtained at different loading factors L_f are shown as examples of the results obtained. The agreement between the calculated and experimental profiles is excellent under all conditions, particularly for the diffuse rear boundaries of these bands.

4.3. Competitive isotherms model

In order to calculate the binary adsorption equilibrium isotherms, the method suggested by the IAS theory was implemented as explained in the Theory section. The implicit set of Eqs. (29)–(35) was solved using the Marquardt routine. Since the experimental data afforded by the perturbation method

Table 3
Values of the parameters used in the GR and TD models

		λ_i (Eq. (35))		
		For single comp.	For mix. 1:1	For mix. $\Sigma c_i = 15$ (g/l^3)
Total porosity ε_t	$\varepsilon_t^0 = 0.61$	4.47e−3	4.38	4.86e−4
Pore porosity ε_p	$\varepsilon_p^0 = 0.381$	7.07e−3	6.98	7.64e−4
External porosity ε_e [38]		0.37		
Tortuosity θ^0		6.88		
F^0		0.639		
F_e		1.703		
Dispersion coefficient D_L (cm^2/s) [42]		$1.0 \cdot 10^{-5}$		
Molecular diffusivity $D_{m,i}$ (cm^2/s) [41]	Comp. (1) $5.46 \cdot 10^{-5}$		Comp. (2) $4.74 \cdot 10^{-5}$	

are the retention times of the perturbation pulses, the results of the IAS theory were converted into retention times of these pulses. The partial derivatives necessary for the calculations were determined numerically for each pair of concentrations.

The results of these calculations are illustrated in Fig. 4a and b for the 1:1 mixture and in Fig. 5 for the mixtures with $C_1 + C_2 = 15$ g/l. The plot of the calculated retention times of the pulses versus the plateau concentrations matches well the corresponding plot of the experimental retention times for

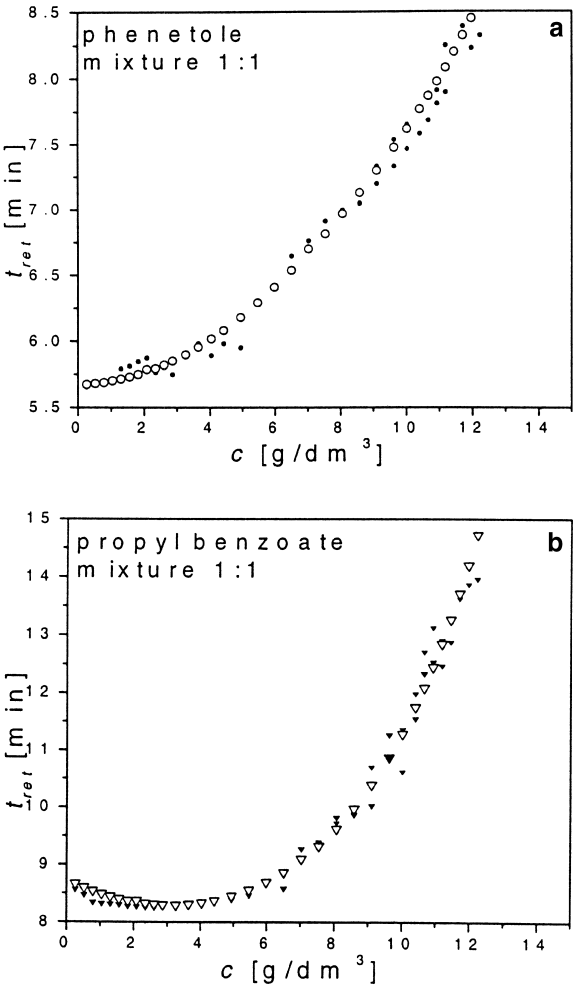

Fig. 4. Validation of the competitive isotherm data. Retention time of the perturbations as a function of the plateau concentration. Solid symbols, experimental data; empty symbols, calculation using the IAS method and the coherence condition. 1:1 Mixtures. (a) Phenetole. (b) Propyl benzoate.

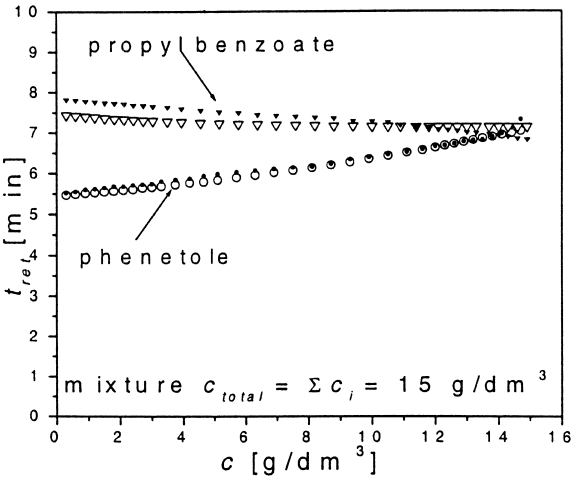

Fig. 5. Validation of the competitive isotherm data. Retention time of the perturbations as a function of the plateau concentration. Solid symbols, experimental data; empty symbols, calculation using the IAS method and the coherence condition. Mixtures with $C_1 + C_2 = 15$ g/l.

the 1:1 mixture and for the $C_1 + C_2 = 15$ g/l mixtures, although there is an obvious small but systematic discrepancy for propyl benzoate (Fig. 5). These discrepancies can be explained by the complex mechanism of arranging the molecules of two solutes (that have slightly different geometrical dimensions) on the different adsorption layers. The geometric rule assumed is too simple for providing the perfect agreement. However, the further introduction of solid-phase activity coefficients was considered as artificial given the assumption already made in combining two multilayer isotherms, which already take into the phase non-ideal behavior.

In conclusion, the agreement observed between the calculated and the experimental isotherm data achieved in the wide range of total and relative concentrations of the two compounds in the mixtures that were studied is extremely satisfactory.

4.4. Validation of the competitive isotherm models

Overloaded band profiles were acquired for a series of binary mixtures of different compositions, under experimental conditions that were varied systematically. The experimental conditions used are summarized in Table 4 (only part of the data acquired is illustrated in the figures shown). The

Table 4
Parameters of overloaded peaks

No.	Mixture	Inlet concentration		Inlet mole fraction		Injection time	Loading factor	
		$c_{(1)}$ (g/l)	$c_{(2)}$ (g/l)	(1)	(2)	t_{inj} (min)	$L_{f(1)}$	$L_{f(2)}$
1a	1:2	1.77	3.79	0.20	0.33	0.5	0.004	0.013
1b				0.40	0.66	1	0.009	0.025
1c				0.80	1.32	2	0.018	0.050
1d				1.00	1.65	2.5	0.023	0.063
2a		2.62	5.61	0.30	0.48	0.5	0.006	0.019
2b				0.60	0.96	1	0.013	0.037
2c				1.20	1.92	2	0.026	0.074
2d				1.50	2.40	2.5	0.033	0.093
3a		3.40	7.28	0.39	0.63	0.5	0.008	0.024
3b				0.78	1.26	1	0.017	0.048
3c				1.56	2.52	2	0.034	0.096
3d				1.95	3.15	2.5	0.043	0.120
4a		5.24	11.22	0.60	0.96	0.5	0.013	0.037
4b				1.20	1.92	1	0.026	0.074
4c				2.40	3.84	2	0.052	0.148
4d				3.00	4.80	2.5	0.065	0.185
5a		6.80	14.55	0.785	1.25	0.5	0.017	0.048
5b				1.57	2.5	1	0.033	0.096
5c				3.14	5	2	0.066	0.192
5d				3.925	6.25	2.5	0.083	0.240
1a	1:1	3.14	3.14	0.36	0.27	0.5	0.008	0.010
1b				0.72	0.54	1	0.015	0.021
1c				1.44	1.08	2	0.031	0.041
1d				1.80	1.35	2.5	0.038	0.052
2a		4.65	4.65	0.54	0.40	0.5	0.011	0.015
2b				1.08	0.80	1	0.023	0.031
2c				2.16	1.60	2	0.046	0.061
2d				2.70	2.00	2.5	0.057	0.077
3a		6.03	6.03	0.70	0.52	0.5	0.015	0.020
3b				1.40	1.04	1	0.030	0.040
3c				2.80	2.08	2	0.059	0.080
3d				3.50	2.60	2.5	0.074	0.099
4a		9.29	9.29	1.07	0.80	0.5	0.023	0.031
4b				2.14	1.60	1	0.046	0.061
4c				4.28	3.20	2	0.091	0.123
4d				5.35	4.00	2.5	0.110	0.153
5a		12.06	12.06	1.39	1.04	0.5	0.030	0.040
5b				2.78	2.08	1	0.059	0.080
5c				5.56	4.16	2	0.118	0.159
5d				6.95	5.20	2.5	0.148	0.199

Table 4. Continued

No.	Mixture	Inlet concentration		Inlet mole fraction		Injection time	Loading factor	
		$c_{(1)}$ (g/l)	$c_{(2)}$ (g/l)	(1)	(2)	t_{inj} (min)	$L_{f(1)}$	$L_{f(2)}$
3a	1:1	7.23	3.88	0.84	0.33	0.5	0.018	0.013
3b				1.68	0.66	1	0.035	0.026
3c				3.36	1.32	2	0.071	0.051
3d				4.20	1.65	2.5	0.089	0.064
4a		10.70	5.74	1.24	0.49	0.5	0.026	0.019
4b				2.48	0.98	1	0.052	0.038
4c				4.96	1.96	2	0.105	0.076
4d				6.20	2.45	2.5	0.131	0.095
5a		13.88	7.50	1.60	0.64	0.5	0.034	0.025
5b				3.20	1.28	1	0.068	0.050
5c				6.40	2.56	2	0.136	0.099
5d				8.00	3.20	2.5	0.170	0.124

profiles recorded were compared to those calculated with the modified TD model, coupled with the IAS competitive isotherm model based on the two single-component BET isotherms. The investigation of these band profiles indicates that, at low values of the loading factor, the bands of the two components of the binary mixtures behave independently and in a manner similar to the bands of single-component mixtures. This was expected since, under such conditions, the bands are well and rapidly separated, so they travel along the column independently. Such an independent behavior of the bands was found for the following values of the loading factors:

(a) For 1:2 mixtures, $L_{f,1} < 0.026$ and $L_{f,2} < 0.074$; samples 1a,b; 2a,b; 3a,b; 4a,b; 5a; see first part of Table 4;
(b) For 1:1 mixtures, $L_{f,1} < 0.03$ and $L_{f,2} < 0.04$; samples 1a,b; 2a,b; 3a,b; 4a; 5a; see middle part of Table 4;
(c) For 2:1 mixtures, $L_{f,1} < 0.02$ and $L_{f,2} < 0.01$; samples 3a; see last part of Table 4.

Typical profiles illustrating these results are shown in Fig. 6a and b that correspond to cases 3a (first part of Table 4) and 3b (middle part of Table 4), respectively. These results are in agreement with the classical results regarding the range of the grey area separating linear from non-linear chromatography behavior [1].

For higher loading factors complete separation of the bands can no longer be achieved and the effects of the competition between the two components can be observed:

(a) Samples 1c,d; 2c,d; 3c,d; 4c,d; 5b,c,d for mixture 1:2;
(b) Samples 1c,d; 2c,d; 3c,d; 4b,c,d; 5b,c,d for mixture 1:1;
(c) Samples 3b,c,d; 4a,b,c,d; 5a,b,c,d for mixture 2:1.

Since in these cases our non-selective detector provides a signal that is related to the sum of the concentrations of the two components in the mixed zones in which the two bands overlap, it is not possible to determine the elution profiles of the two compounds without fraction collection. Instead, we calculated the UV signal corresponding to the band profiles obtained as numerical solutions of the computer program. This was done by reversing the calibration curves of the detector, $\mathrm{mAU} = f(C)$. It was assumed that the signal corresponding to the intermediate, mixed zone was the mere sum of the signals corresponding to each component. Although the signal is nonlinear, the error is small because, in most cases, the deviation from linear behavior is moderate in the concentration range sampled by the mixed zone.

The progressive changes in the band profiles that take place under the influence of an increasing loading factor are illustrated in Figs. 7–10. The strong interaction between the zones of the two components when they interfere is unusual. The

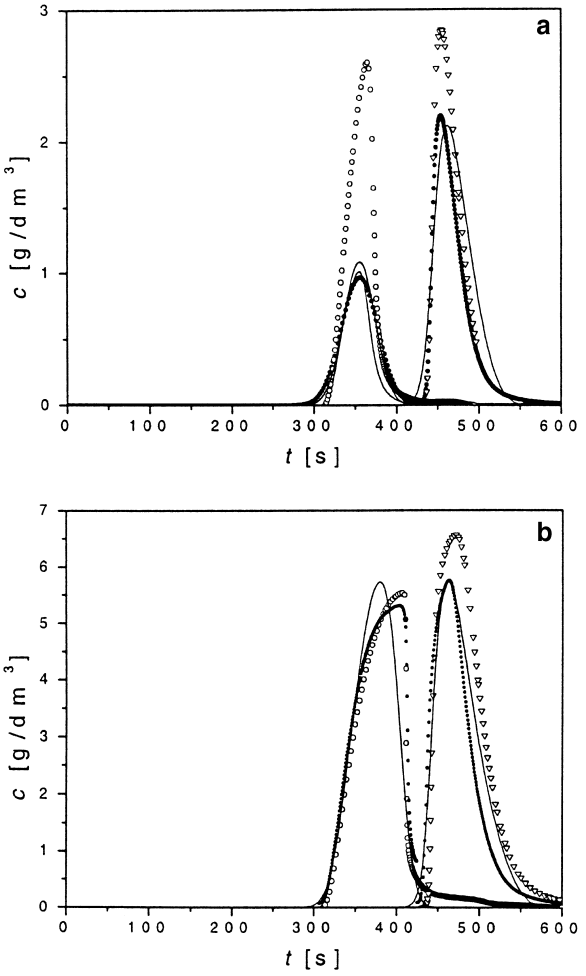

Fig. 6. Comparison between calculated and experimental band profiles for binary mixtures. Validation of the IAS theory. Calculations made with the TD model. Solid symbols, experimental data; solid line, calculated profile. The empty symbols show the single-component band profiles, for the sake of comparison. (a) 1:2 mixture, $C_1 = 3.4$ g/l and $C_2 = 7.28$ g/l; $t_{inj} = 30$ s. (b) 1:1 mixture, $C_1 = 6.03$ g/l and $C_2 = 6.03$ g/l; $t_{inj} = 60$ s.

characteristic displacement effect that takes place in the case of Langmuirian isotherms does not take place here. The component that is first eluted exhibits a self-sharpening rear front (see Fig. 2b). Its presence ahead of the band of the second component inhibits or rather delays the migration of this second band. This effect that is similar to the well known displacement effect but acts in the opposite direction has been called the retainment effect. It has rarely been observed. The progressive evolution of this phenomenon can be observed in Figs. 6–8. The position of the first eluted band remains unchanged, with a retention time similar to the band of the single solute. The main change observed in the shape of

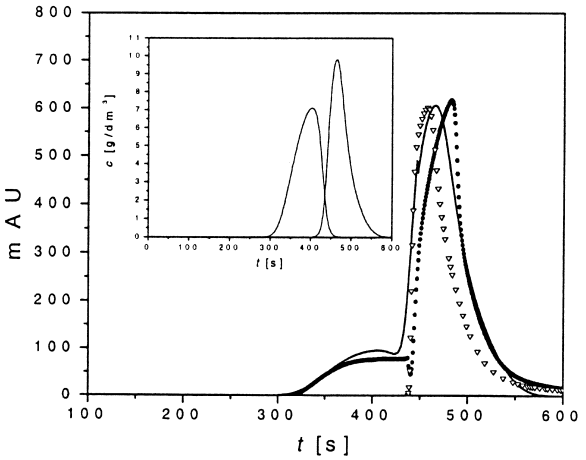

Fig. 7. Comparison between calculated and experimental band profiles for binary mixtures. Validation of the IAS theory. Calculations made with the TD model. Solid symbols, experimental data; solid line, calculated profile. The empty symbols show the single-component band profile of component 2, for the sake of comparison. 1:1 mixture, $C_1 = 9.28$ g/l and $C_2 = 9.28$ g/l; $t_{inj} = 60$ s.

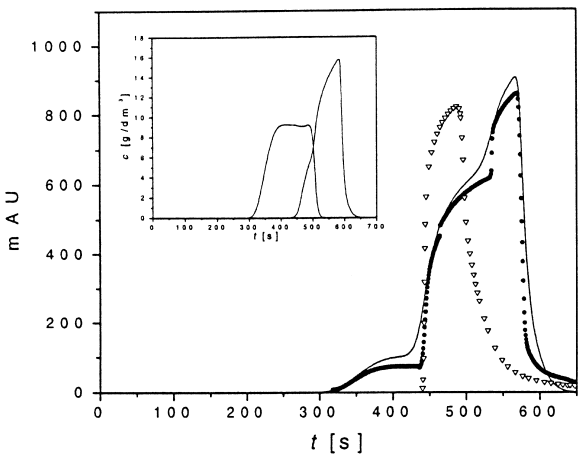

Fig. 8. Comparison between calculated and experimental band profiles for binary mixtures. Validation of the IAS theory. Calculations made with the TD model. Solid symbols, experimental data; solid line, calculated profile. The empty symbols show the single-component band profile of component 2, for the sake of comparison. Inset, calculated individual profiles. 1:1 mixture, $C_1 = 12.08$ g/l and $C_2 = 12.08$ g/l; $t_{inj} = 120$ s.

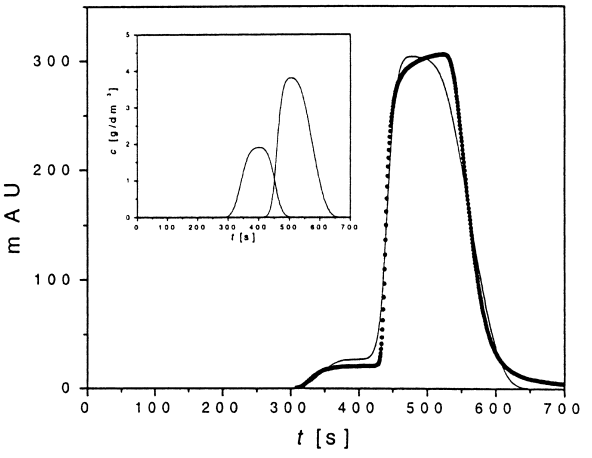

Fig. 9. Comparison between calculated and experimental band profiles for binary mixtures. Validation of the IAS theory. Calculations made with the TD model. Solid symbols, experimental data; solid line, calculated profile. Inset, calculated individual profiles. 1:1 mixture, $C_1 = 1.77$ g/l and $C_2 = 3.79$ g/l; $t_{inj} = 120$ s.

this band with increasing loading factor is the lengthening of its plateau.

5. Conclusions

The agreement between the experimental and calculated band profiles confirms the competitive multilayer adsorption isotherm behavior that was demonstrated for the two compounds studied. This agreement persists even when a simple chromatographic model such as the TD model is used to calculate the band profiles, because the mass transfer kinetics of these simple, low molecular mass, weakly polar compounds is rather fast, rendering minor the contribution of the mass transfer resistances to the profiles of their bands. In cases like this one, computer-assisted optimization of a separation process would be straightforward. It would be impossible if a Langmuir model were to be forced on the data.

This work suggests that, when the adsorption behaviors of two compounds follow the same isotherm model, the IAS theory is an excellent approach to derive for them a set of competitive isotherms. This result might have great practical importance. It was not obvious and it needs to be confirmed. It seems that it would not apply when the two compounds exhibit isotherm behaviors that are in markedly qualitative contrast, leading to different isotherm models for their single-component isotherm data [42]. This agreement was obtained in a wide range of loading factors, between 0.2 and 20%. The small discrepancies that are observed can be explained by the complexity of the multilayer adsorption of the molecules of a mixture with different sizes and molecular interactions on the one hand, by the difficulties in accounting exactly for the signal that is given by an overloaded UV detector when it responds to a mixture.

The combination of FA measurements to acquire the single-component isotherm data and of perturbation measurements to acquire sets of competitive isotherm data might be an improvement over the use of competitive FA measurements. The success of this combination of experimental methods in this work is largely due, however, to the fact that the competitive isotherm model derived from the two single-component isotherms by the IAS method was itself successful in accounting for the competitive adsorption behavior of the two compounds. The main drawback of the perturbation method compared to FA remains that the a priori selection of a model is required, so that the data can be fitted to that model.

Finally, the chromatograms obtained for the two

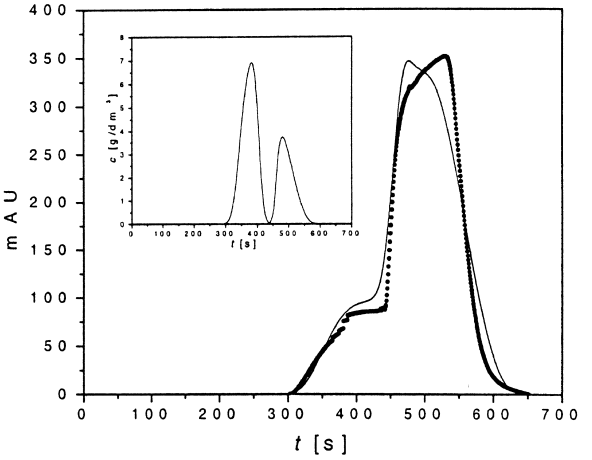

Fig. 10. Comparison between calculated and experimental band profiles for binary mixtures. Validation of the IAS theory. Calculations made with the TD model. Solid symbols, experimental data; solid line, calculated profile. Inset, calculated individual profiles. 1:1 mixture, $C_1 = 7.23$ g/l and $C_2 = 3.88$ g/l; $t_{inj} = 120$ s.

compounds studied here provide a rare example of an unusual type of band interaction, the retainment effect. Since, at high loading factors, each one of the two bands has its self-sharpening front directed toward the other one, the production rate achieved in their separation should be unusually large if it were a situation of practical relevance.

Acknowledgements

This work was supported in part by grant CHE-00-70548 from the National Science Foundation, by the cooperative agreement between the University of Tennessee and the Oak Ridge National Laboratory, and by grant 4T09C02624 of the Polish State Committee for Scientific Research.

References

[1] G. Guiochon, S. Golshan-Shirazi, A.M. Katti, Fundamentals of Preparative and Nonlinear Chromatography, Academic Press, Boston, MA, 1994.
[2] G. Ganetsos, P. Barker, Preparative and Production Scale Chromatography, Marcel Dekker, New York, 1993.
[3] D.M. Ruthven, Principles of Adsorption and Adsorption Process, Wiley, New York, 1984.
[4] C.B. Ching, K.H. Chu, D.M. Ruthven, AIChE J. 36 (1990) 275.
[5] C. Blümel, P. Hugo, A. Seidel-Morgenstern, J. Chromatogr. A 865 (1999) 51.
[6] F. Gritti, W. Piatkowski, G. Guiochon, J. Chromatogr. A 978 (2002) 81.
[7] F. Gritti, W. Piatkowski, G. Guiochon, J. Chromatogr. A 983 (2003) 51.
[8] W. Piatkowski, F. Gritti, K. Kaczmarski, G. Guiochon, J. Chromatogr. A 989 (2003) 207.
[9] C.J. Radke, J.M. Prausnitz, AIChE J. 18 (1972) 761.
[10] A.L. Myers, J.M. Prausnitz, AIChE J. 11 (1965) 121.
[11] E.V. Dose, S. Jacobson, G. Guiochon, Anal. Chem. 63 (1991) 833.
[12] F.G. Helfferich, R.D. Withley, J. Chromatogr. A 734 (1996) 7.
[13] A. Seidel-Morgenstern, G. Guiochon, AIChE 48 (1993) 2787.
[14] K. Kaczmarski, D. Antos, J. Chromatogr. A 756 (1996) 73.
[15] K. Kaczmarski, D. Antos, H. Sajonz, P. Sajonz, G. Guiochon, J. Chromatogr. A 925 (2001) 1.
[16] W. Piatkowski, D. Antos, K. Kaczmarski, J. Chromatogr. A, submitted for publication.
[17] D. Gunn, Chem. Eng. Sci. 42 (1987) 363.
[18] M. Suzuki, Adsorption Engineering, Elsevier, Amsterdam, 1990.
[19] M.W. Phillips, G. Subramanian, S.M. Cramer, J. Chromatogr. 454 (1988) 1.
[20] S. Golshan-Shirazi, B. Lin, G. Guiochon, J. Phys. Chem. 93 (1989) 6871.
[21] K. Kaczmarski, D. Antos, J. Chromatogr. A 756 (1999) 1.
[22] L. Lapidus, N.L. Amundson, J. Phys. Chem. 56 (1952) 984.
[23] D. Antos, K. Kaczmarski, W. Piatkowski, A. Seidel-Morgenstern, J. Chromatogr. A, submitted for publication.
[24] D. Antos, Habilitation Thesis, Otto-von-Guericke Universität, Magdeburg, 2003.
[25] S. Brunauer, P.H. Emmet, E. Teller, J. Am. Chem. Soc. 60 (1938) 309.
[26] D.M. Youg, A.D. Crowell, Physical Adsorption of Gases, Butterworths, London, UK, 1962.
[27] C.N. Reilley, G.P. Hildebrand, J.W. Ashley Jr., Anal. Chem. 34 (1962) 1198.
[28] F.G. Helfferich, P.W. Carr, J. Chromatogr. 629 (1993) 97.
[29] F.G. Helfferich, G. Klein, Multicomponent Chromatography, Marcel Dekker, New York, NY, 1970.
[30] V. Gusev, J. O'Brien, C.R.C. Jensen, N.A. Seaton, AIChE J. 42 (1996) 2773.
[31] K. Kaczmarski, M. Mazotti, G. Storti, M. Morbidelli, Comp. Chem. Eng. 21 (1997) 641.
[32] V.J. Villadsen, M.L. Michelsen, Solution of Differential Equation Model by Polynomial Approximation, Prentice–Hall, Englewood Cliffs, NJ, 1978.
[33] R.T. Yang, J.B. Fenn, G.L. Haller, AIChE J. 19 (1973) 1052.
[34] P.N. Brown, A.C. Hindmarsh, G.D. Byrne, Variable-Coefficient Ordinary Differential Equation Solver, procedure available at http://www.netlib.org
[35] D.W. Marquardt, SIAM J. Appl. Math. 11 (1963) 431.
[36] M. Kele, G. Guiochon, J. Chromatogr. A 960 (2002) 19.
[37] M. Al-Bokari, D. Cherrak, G. Guiochon, J. Chromatogr. A 975 (2002) 275.
[38] S. Golshan-Shirazi, G. Guiochon, J. Chromatogr. 506 (1990) 495.
[39] A.L. Myers, AIChE J. 29 (1983) 691.
[40] C.R. Wilke, P. Chang, AICHE J. 1 (1955) 264.
[41] D. Gunn, Chem. Eng. Sci. 42 (1987) 363.
[42] A. Seidel-Morgenstern, G. Guiochon, Chem. Eng. Sci. 48 (1993) 2787.